Enhanced Photoluminescence and Thermal Stability of Zinc Quinolate Following Complexation on the Surface of Quantum Dot

Satyapriya Bhandari[a], Shilaj Roy[b] and Arun Chattopadhyay[a,b,*]

[a] Department of Chemistry, [b] Centre for Nanotechnology

Indian Institute of Technology Guwahati

Assam-781039, India

*Email: arun@iitg.ernet.in

†Electronic Supplementary Information

Experimental details

A. Materials

8-Hydroxyquinoline (HQ, Merck), zinc acetate dihydrate (99%, Merck), sodium sulphide (58%, Merck), sodium hydroxide (Merck), L- cysteine hydrochloride (Loba Chemie, India), methanol (Merck), methanol (HPLC), potassium bromide (Sigma Aldrich), quinine sulphate were used as received without further purification. Mili-Q grade water was used in all experiments.

B. Synthesis and characterization of ZnS quantum dots

L-cysteine stabilized ZnS quantum dots (Qdots) were synthesized by an aqueous chemical precipitation method. To synthesize the Qdots, 5.0 mM of zinc acetate dihydrate, 5.0 mM of sodium sulphide and 5.0 mM of L-cysteine hydrochloride were taken in a round bottom flask containing 50 mL of Mili Q grade water. At first, zinc acetate dihydrate was dissolved in 30 mL of water and to that solution 10 mL of 25.0 mM sodium sulphide and 10 ml of 25.0 mM cysteine hydrochloride solution (with pH adjusted to ~11 by adding 0.8 M NaOH) were added simultaneously under constant stirring. The resulting mixture turned milky white in color and was refluxed for 3 h under constant stirring at 100 ^{o}C. Finally, the milky white colloidal dispersion so obtained was centrifuged at a speed of 25,000 rpm for 15 min; the pellet was washed with water, redispersed in 50 mL water and the same cycle was repeated. The pellet obtained (after centrifugation twice) was dispersed in 100 mL water following sonication for 10 min. The dispersion was used for further experiments. The same procedure was followed to synthesize uncapped ZnS Qdots instead of using cysteine (except that the mixture was refluxed for half an hour at 100 ^{0}C in order to avoid much agglomeration). The synthesized Qdots were

characterized using X-ray diffraction (XRD), transmission electron microscopy (TEM), high resolution TEM (HRTEM), UV-Vis, photoluminescence (PL) and FTIR spectroscopy.

The powder X-ray diffraction (XRD) pattern of the as-synthesized precipitates of both capped and uncapped Qdots exhibited three prominent peaks at 28.6^o, 47.9^o and 56.5^o (Figure S18A-B). The three characteristic peaks are due to the (111), (220) and (311) planes of the cubic ZnS Qdots.[1-2] The morphology of ZnS Qdots can be observed on TEM images in Figure S15A and S19 with average particle size 3.2 + 0.5 nm (for capped Qdots) and 4.0 + 0.5 nm (for uncapped Qdots). Further, selected area electron diffraction (SAED) confirmed the crystalline nature of the Qdots (Figure S14A). The internal lattice fringes (d_{sp} = 0.3 nm; indicating 111 plane of ZnS) observed for capped Qdots in HRTEM (Figure S14A) also confirmed the formation of cubic ZnS Qdots. [1-2] Figure S20 (A-B) shows absorption and emission spectra of ZnS Qdot dispersion. While absorption spectrum showed an edge at 308 nm for the capped one and at 318 nm for uncapped one, the emission spectrum (λ_{ex} = 322 nm) exhibited broad emission band centered at 440 nm for both Qdots. [1-2] Presence of cysteine on the surface of the Qdots was confirmed by FTIR spectroscopy and absence of –S-H bands in Qdots confirmed that cysteine binds the Qdots through –S atom of thiol group of cysteine for capped ZnS Qdots (Figure S21).

C. Preparation of Ligand (HQ) Solutions:

5.0 mM 8-hydroxy quinoline (HQ) solution in methanol was prepared using sonication.

D. Synthesis and Characterization of $ZnQ_2.2H_2O$ Complex:

The $ZnQ_2.2H_2O$ complex was prepared by using a sonochemical method. 5.0 mM HQ was dissolved in 10 mL of methanol and then it was added drop-wise to 10.0 mM of 10.0 mL zinc acetate solution (in water) which was followed by sonication for an hour. Finally, the yellowish green precipitate so obtained was filtered out and repeatedly washed with MiliQ water and

hexane to remove unreacted metal salts and ligand respectively. The final products were dried under room temperature and were used for further experiments. The synthesized complex was characterized using XRD, UV-Vis, FTIR and PL spectroscopy, SEM and optical microscopic analysis.

The powder XRD pattern of the as-synthesized precipitates exhibited two strongest peaks at 6.9^{o} and 20.8^{o}, which indicated the formation of $ZnQ_2.2H_2O$ complex (Figure S22A). Scanning electron microscopic analysis revealed known rod-like shape of the complex (Figure S22B).[3-4] Figure S23A shows the optical absorption and emission spectra of complex in methanol. $ZnQ_2.2H_2O$ complex shows broad absorption maximum at 380 nm which arises from efficient ligand to metal transfer and its broadness depends upon the transition populating ligand centered excited states. On the other hand, emission of the complex was observed at 550 nm and is due to a transition from electron rich phenoxide ring (HOMO; highest occupied molecular orbital) to the electron deficient pyridyl ring (LUMO; lowest occupied molecular orbital). The nature of photoluminescence of complex depends upon the coordination and angle of the ligand and presence of additional functional group. As for example, introduction of electron withdrawing groups in phenoxide and pyridyl ring causes blue shifts and red shifts respectively in the emission of the AlQ_3 complex while electron donating groups shows the reverse effect. [5-6]

The presence of HQ and water of hydration in the zinc quinolato complex was verified by FTIR spectroscopy (Figure S23B and also refer to the expanded FTIR spectra in Figure 26-27). Figure 2 (manuscript) shows the TGA and DSC results of the complex. In TGA, two step weight loss was observed; first one occurred from 120 ^{o}C upto 150 ^{o}C and second one at 450 ^{o}C, while DSC curve shows endothermic peaks at 160 ^{o}C and at 360 ^{o}C. The first weight loss is ascribed to loss of coordinated two water molecules while second one indicates the decomposition of the

complex in the TGA curve. Water loss and decomposition of the complex were further confirmed by observing two endothermic peaks - one at 160 ^{o}C and another sharp peak at 360 ^{o}C respectively in the DSC curve.[3] The presented results clearly indicated the formation of $ZnQ_2.2H_2O$.

E. Synthesis and characterization of QDCs

Room temperature synthesis of QDC was carried out by the following two steps.

I) To 2 mL of cysteine capped ZnS (pH-6.6) Qdot water dispersion (with an absorption value of 0.03 at 361 nm), 2 μL methanolic solution of 5.0 mM HQ was added step-wise. The fluorescence spectrum of the Qdots in the presence of the ligand was monitored with spectrofluorimeter. The optimum concentration of ligand was taken as the concentration at which the resultant mixture showed maximum emission intensity at its peak. (Figure S24) Similar fluorimetric titration was carried out using 0.5 mM methanolic solution of $ZnQ_2.2H_2O$ complex. (Figure S25) The optimum amount of ligand and complex added to 2 mL Qdots dispersion were 30 μL and 100 μL, respectively.

II) After separate addition of optimum amount of ligand and complex to 2 mL of Qdot dispersions, the resulting solutions were centrifuged with a speed of 25000 rpm for 15 min. The obtained supernatant and pellet (after being redispersed into same amount of solvent) were used for PL spectroscopy to check the attachment behavior of HQ and complex. The cycle of centrifugation and redispersion of the dispersion from pellet was repeated until supernatant was nonfluorescent at the same excitation wavelength. The final pellet was collected and was redispersed into the same amount of solvent (2mL) which was then used for UV-Vis, PL, TRPL spectroscopic measurements and TEM analysis. The pH of the medium of both the QDC dispersions (either from HQ added or ZnQ_2 added Qdots) before and after centrifugation

remained unchanged from the dispersion of as-synthesized Qdots (pH-6.6). The powder XRD, TGA, DSC, FTIR and optical microscopic analysis of QDCs were carried out using solid pellet obtained similarly. The PL quantum yields (QY) was measured using quinine sulphate solution (in 0.1 M H_2SO_4) as reference. The photostability of QDC was measured under continuous irradiation of light, using rhodamine 6G as standard dye solutions.

F. Control experiments

I) Formation of QDCs with uncapped ZnS

To 2 mL of uncapped ZnS Qdot dispersion in water, 30.0 μL of 5.0 mM HQ (in methanol) and 0.5 mM $ZnQ_2.2H_2O$ complex in methanol were separately added and the resulting mixtures were centrifuged. The pellet obtained after centrifugation was redispersed into the same amount of solvent to monitor the spectroscopic changes in UV-Vis and PL.

II) Effect of sulphide ions and solvent on the optical properties of $ZnQ_2.2H_2O$ complex

To 2 mL of 0.5 mM methanolic $ZnQ_2.2H_2O$ solution, a pinch of solid Na_2S dissolved in methanol was added. Separately, different amount of 0.5 mM methanolic $ZnQ_2.2H_2O$ was added to 2 mL of water. For both the solutions, UV-Vis and fluorescence measurements were made in order to observe spectroscopic changes.

III) Effect of benzoquinone (BQ) on Qdots/ QDC/ $ZnQ_2.2H_2O$ complex:

To 2.0 mL of cysteine capped ZnS Qdot dispersion in water, 30.0 μL of 5.0 mM BQ (in methanol) was added, followed by addition of 30.0 μL of 5.0 mM HQ (in methanol). Separately, to 2.0 mL of cysteine capped ZnS Qdot dispersion in water, 30.0 μL of 5.0 mM HQ (in methanol) was added first and then 30.0 μL of 5.0 mM BQ (in methanol) was added. The resulting mixtures were used to monitor the spectroscopic changes in fluorescence. Similarly, to

2 mL of 0.5 mM methanolic ZnQ2.2H2O solution, 30.0 μL and 60.0 μL of 5.0 mM BQ (in methanol) were added to observe the effect of BQ on the fluorescence of the complex.

G. Effect of heating on the luminescence properties of $ZnQ_2.H_2O$ complex and QDCs through microscopic analysis and PL spectroscopy.

Solid $ZnQ_2.2H_2O$ complex and QDCs were placed on glass slides, heated above 270 ^oC over a hot plate for 10 min and then cooled to room temperature. The changes in PL due to heating were observed using optical microscopy (under white and UV light). Then the solids were redispersed into water using sonication in order to measure their PL spectroscopic properties.

Instruments

The XRD patterns for the samples were recorded in a Brucker D2 Phaser X-ray diffractometer (having CuKα radiation at 1.5418Å). UV-Vis and PL spectra recordings were carried out with Hitachi U-2900 spectrophotometer and HORIBA-Fluorolg3 spectrofluorimeter respectively. A JEOL JEM-2100 transmission electron microscope (operated at a maximum accelerating voltage of 200 kV) was used to analyze size, structure (from high resolution TEM images) and nature of samples deposited on formvar-carbon-coated copper grids. Inverse fast Fourier transform (IFFT) images were obtained by using Gatan Digital Micrograph software. FT-IR spectra of solid samples were recorded in a Perkin-Elmer (Model: Spectrum One) spectrophotometer. Time-resolved photoluminescence (TRPL) analyses were performed using Life-Spec-II spectrofluorimeter (Edinburgh Instrument, using Pico Quant 375 nm LASER and 308 LED source). The decay curves were analyzed by FAST software, provided by Edinburgh Instrument along with the fluorescence instrument. Quantum yields of samples were measured using quinine

sulphate (in 0.1 M H_2SO_4) as a standard. Photostability experiments were carried out in a Perkin Elmer LS 55 instrument for ½ h, using Rhodamine 6G as standard. TGA and DSC were recorded by using Perkin Elmer 4000 and Perkin Elmer 6000 instruments respectively. Optical microscopy images under white and UV light (at an excitation wavelength of 350 nm) were recorded by OLYMPUS BX 51 microscope fitted with a digital camera. The pH of the dispersions of QDCs and Qdots was measured using a JENWAY 3510- pH meter.

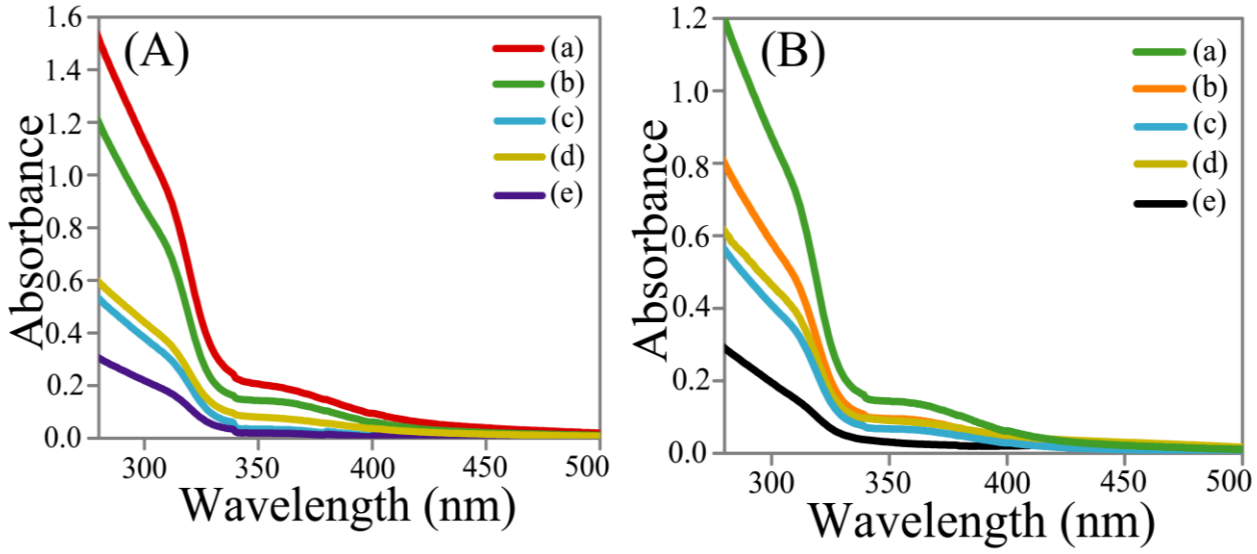

Figure S1. UV-Vis spectra of **(A)** HQ added ZnS Qdots **(B)** ZnQ_2 added ZnS Qdots (a) before centrifugation; (b) pellet (re-dispersed into same amount of solvent) and (c) supernatant after first centrifugation; (d) pellet (re-dispersed into same amount of solvent) and (e) supernatant after second centrifugation.

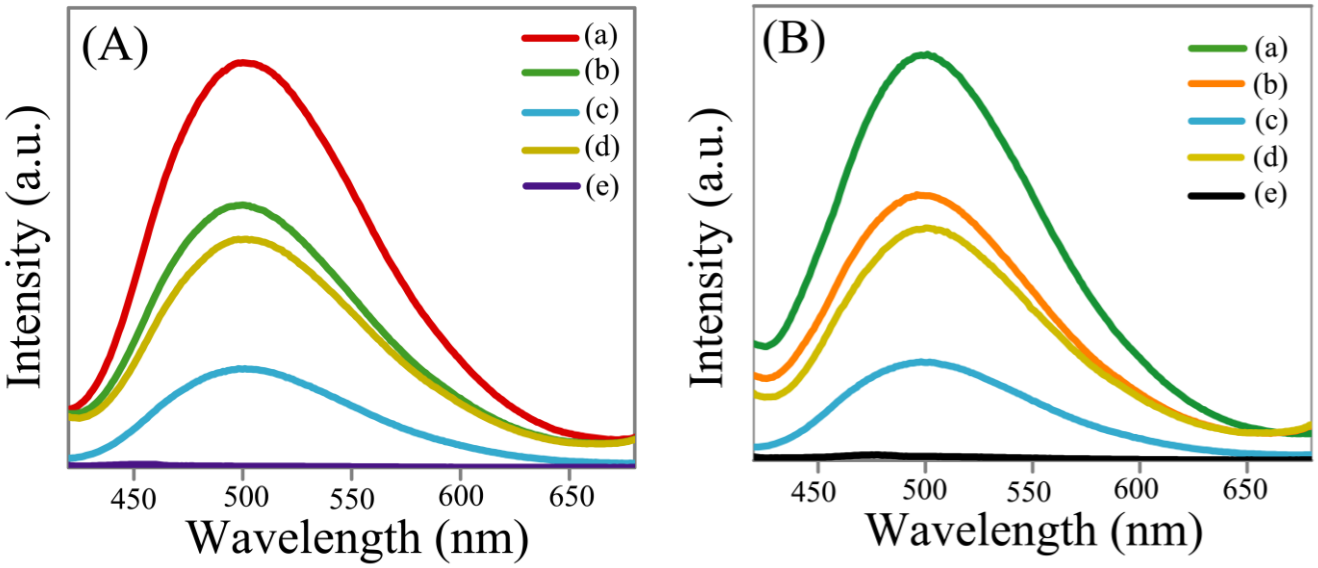

Figure S2. Emission spectra (λ_{ex} = 361nm) of **(A)** HQ added ZnS Qdots **(B)** ZnQ_2 added ZnS Qdots (a) before centrifugation; (b) pellet (re-dispersed into same amount of solvent) and (c) supernatant after first centrifugation; (d) pellet (re-dispersed into same amount of solvent) and (e) supernatant after second centrifugation.

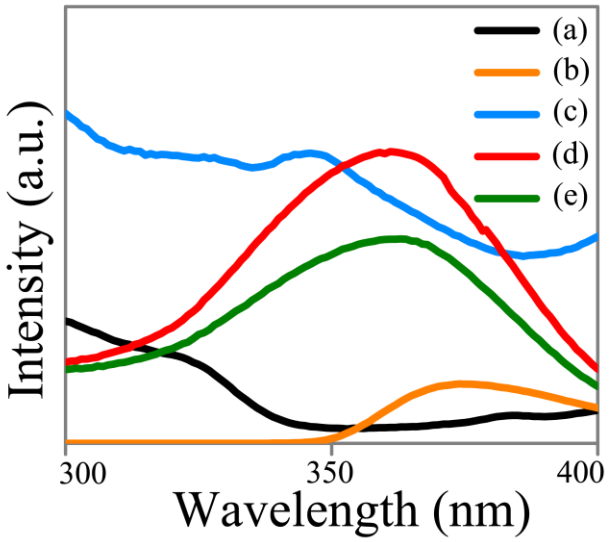

Figure S3. Excitation spectra of (a) cysteine capped ZnS Qdots (λ_{em} = 440 nm); (b) HQ (λ_{em} = 520 nm); (c) ZnQ_2 (λ_{em} = 550 nm); (d) HQ added ZnS Qdots (λ_{em} = 500 nm) and (e) ZnQ_2 added ZnS Qdots and (λ_{em} = 500 nm).

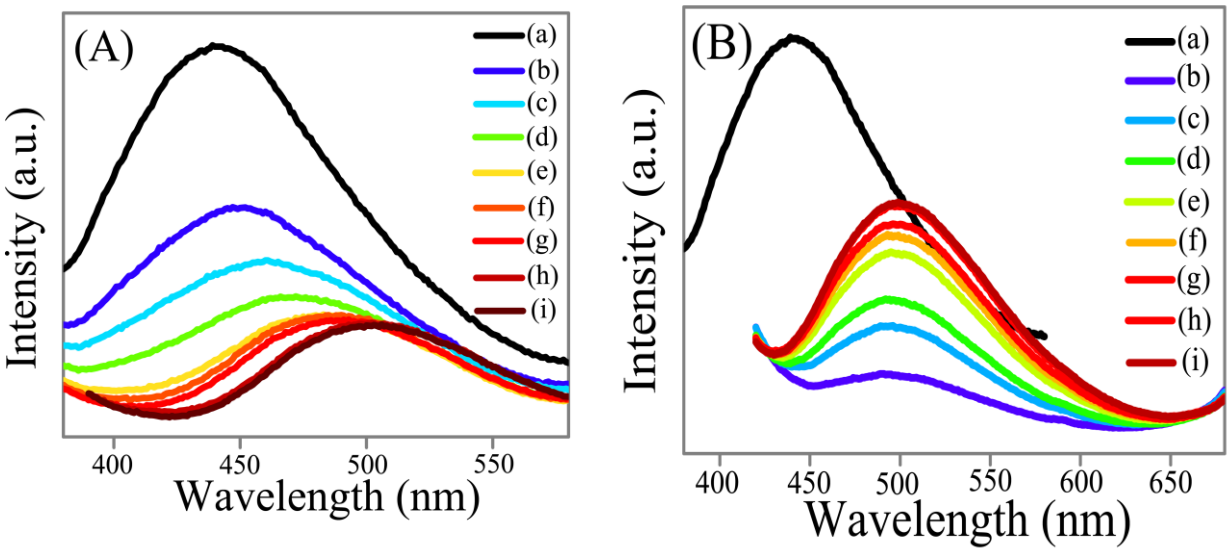

Figure S4. Emission spectra **(A)** at λ_{ex} = 322 nm and **(B)** at λ_{ex} = 361 nm of 2 mL Qdot dispersion in water in the presence of different amounts: (a) 0 µL ; (b) 2.0 µL, **(c)** 4.0 µL, (d) 8.0 µL, (e) 12.0 µL, (f) 16.0 µL, (g) 20.0 µL, (h) 25.0 µL and (i) 30.0 µL respectively, of 1.0 mM HQ (methanol).

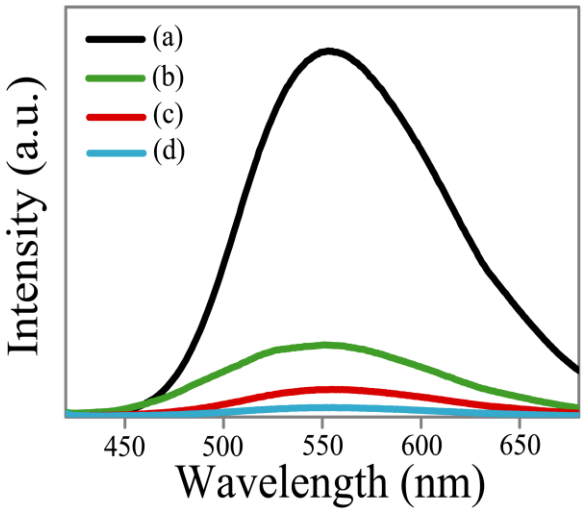

Figure S5. Emission spectra (λ_{ex} = 361 nm) of (a) 0.5 mM of ZnQ_2 complex in methanol; (b) 0.5 mL, (c) 0.2 mL, and (d) 0.1 mL ZnQ_2 complex (in methanol) added to 2 mL of Mili Q water.

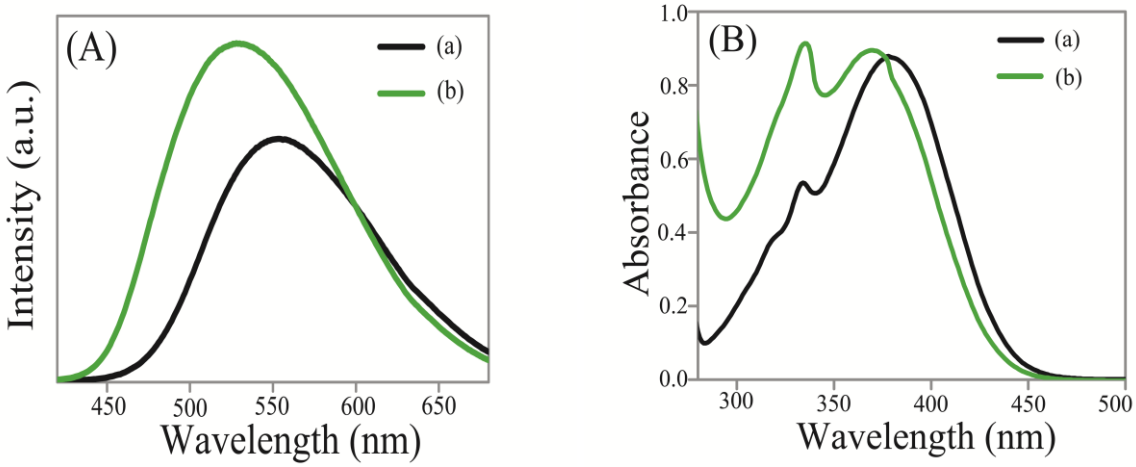

Figure S6. (A) Emission and **(B)** UV-Vis (λ_{ex} = 361 nm) spectra of (a) 0.5 mM of ZnQ_2 complex solution in methanol (pH- 7.4) and (b) that after addition of Na_2S (pH-7.8).

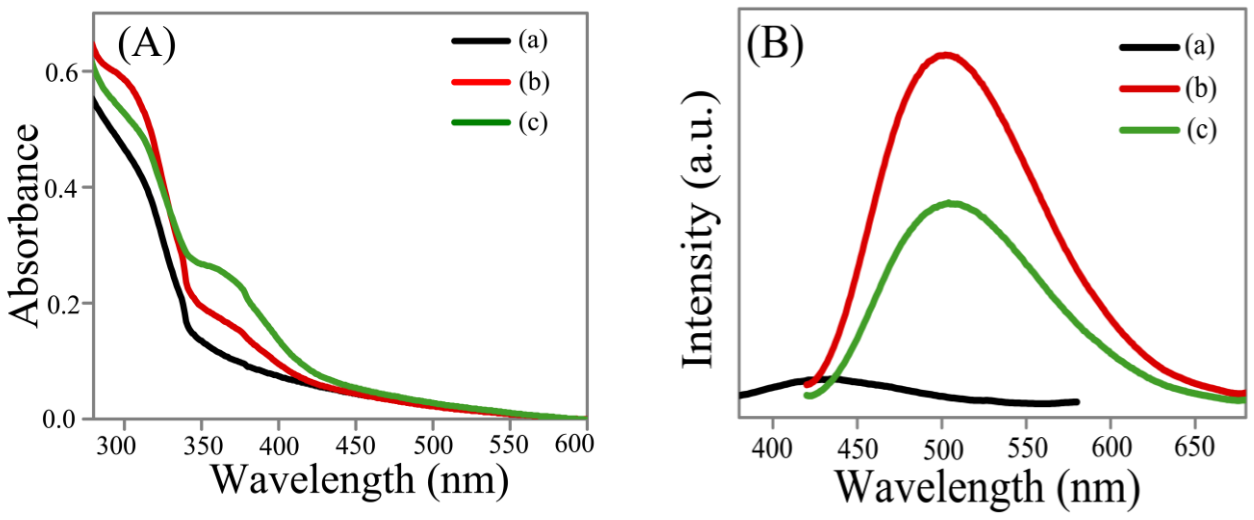

Figure S7. (A) UV-Vis and **(B)** emission spectra of (a) uncapped ZnS Qdots, and of those following addition of (b) 30 μL 5.0 mM HQ (in methanol) and (c) 100 μL of 0.5 mM of ZnQ_2 complex (in methanol) to a 2 mL dispersion in water (emission was monitored at 361nm).

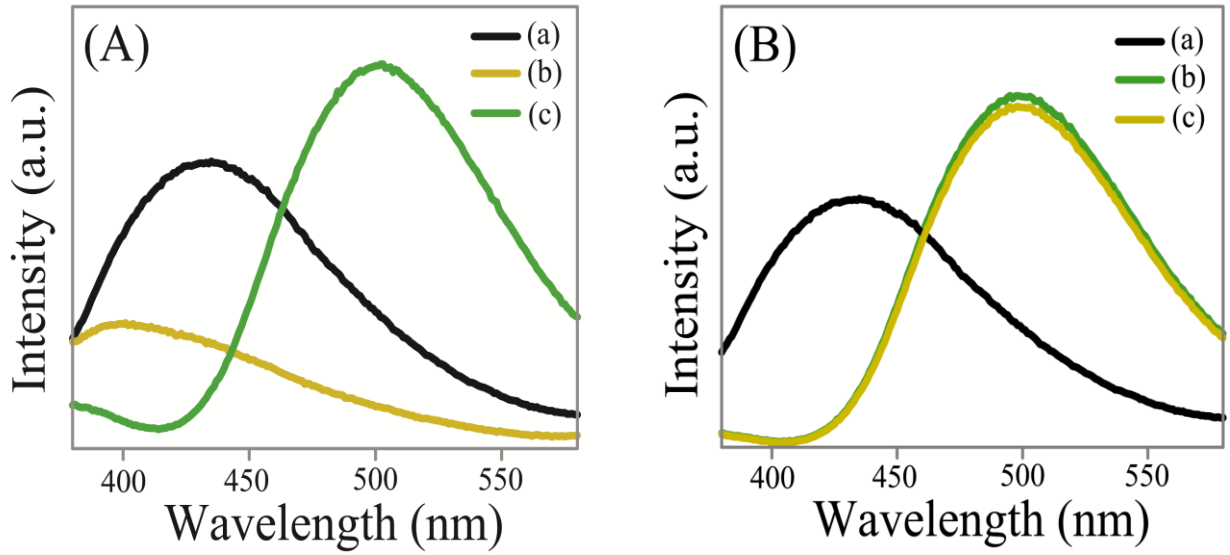

Figure S8. (A) Emission spectra (λ_{ex} = 322 nm) of (a) cysteine stabilized ZnS Qdots (in water), (b) 2.0 mL of ZnS Qdots following addition of 30.0 μL of 5.0 mM BQ and (c) BQ-containing ZnS Qdots to which 30.0 μL of 5.0 mM HQ was then added. **(B)** Emission spectra of (a) cysteine stabilized ZnS Qdots, (b) 2.0 mL of ZnS Qdots following addition of 30.0 μL of 5.0 mM HQ and (c) HQ-containing ZnS Qdots to which 30.0 μL of 5.0 mM BQ was then added.

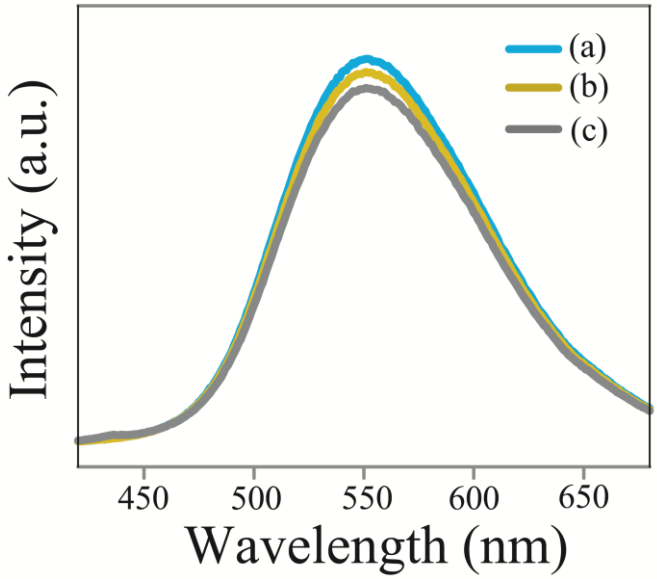

Figure S9. Emission spectra (λ_{ex} = 361 nm) of (a) 2 mL of 0.5 mM ZnQ_2 complex (in methanol) and following addition of (b) 30.0 μL and (c) 60.0 μL 5.0 mM BQ.

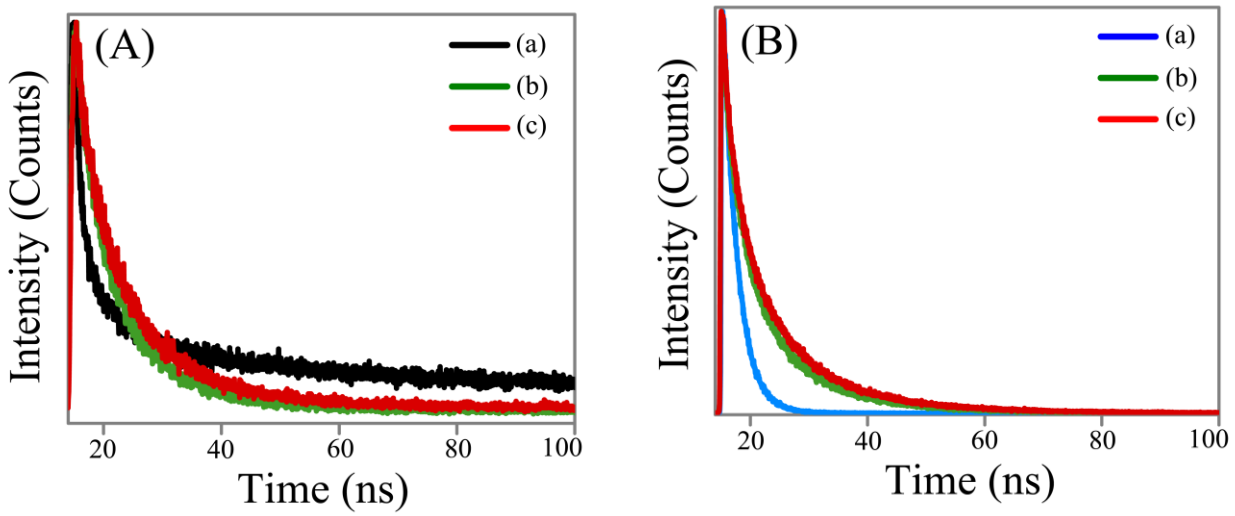

Figure S10. (A) Time-resolved photoluminescence spectra *of* (a) cysteine capped ZnS Qdots; (b) HQ-added ZnS Qdots and (c) ZnQ_2 added ZnS Qdots. The spectra were recorded using LED (308 nm). **(B)** Time-resolved photoluminescence spectra *of* (a) ZnQ_2; (b) HQ-added ZnS Qdots and (c) ZnQ_2 added ZnS Qdots. The spectra were recorded using LASER (375 nm).

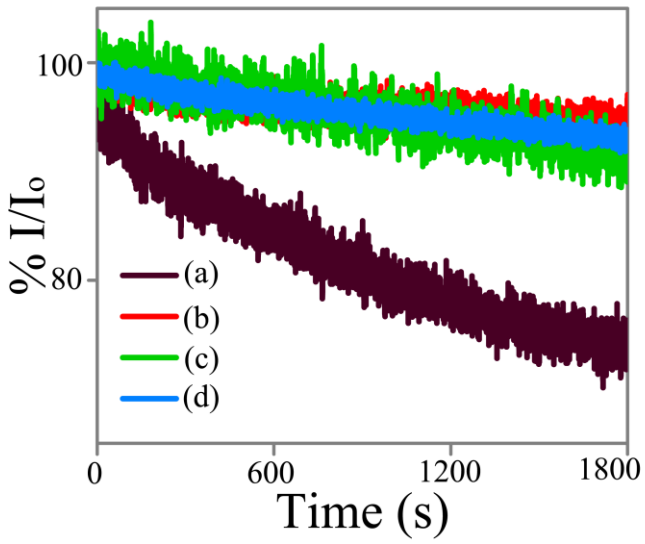

Figure S11. Effect of photo irradiation with time on the emission (λ_{ex} = 361nm) intensity of (a) conventional dye (Rhodamine- 6G); (b) HQ-added ZnS Qdots and (c) ZnQ_2 added ZnS Qdots and (d) ZnQ_2 monitored at their respective emission maximum. The same light was used for irradiation and monitoring of the spectra.

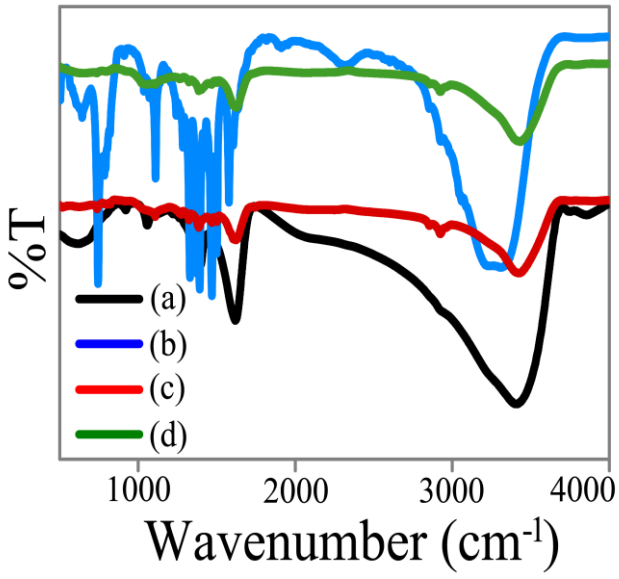

Figure S12. FTIR spectra of (a) cysteine capped ZnS Qdots; (b) ZnQ_2; (c) HQ added ZnS Qdots (d) ZnQ_2 added ZnS Qdots.

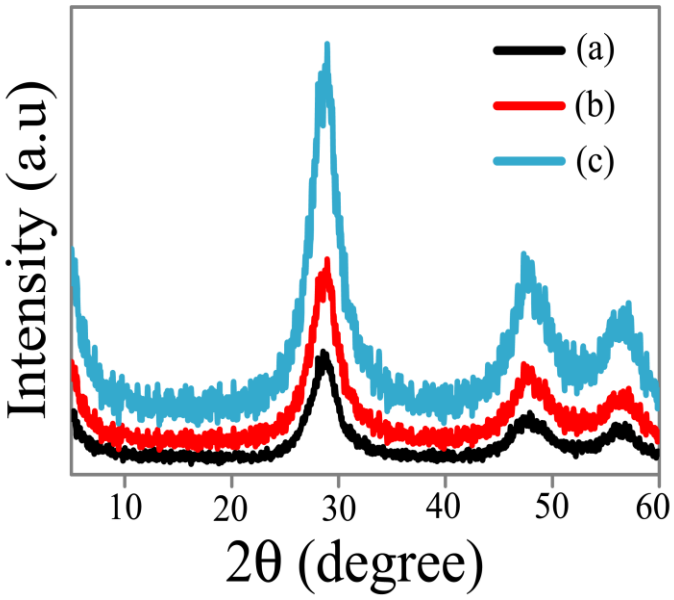

Figure S13. Powder X-ray diffraction pattern of (a) cysteine capped ZnS Qdots; (b) HQ added ZnS Qdots and (c) ZnQ_2 added ZnS Qdots.

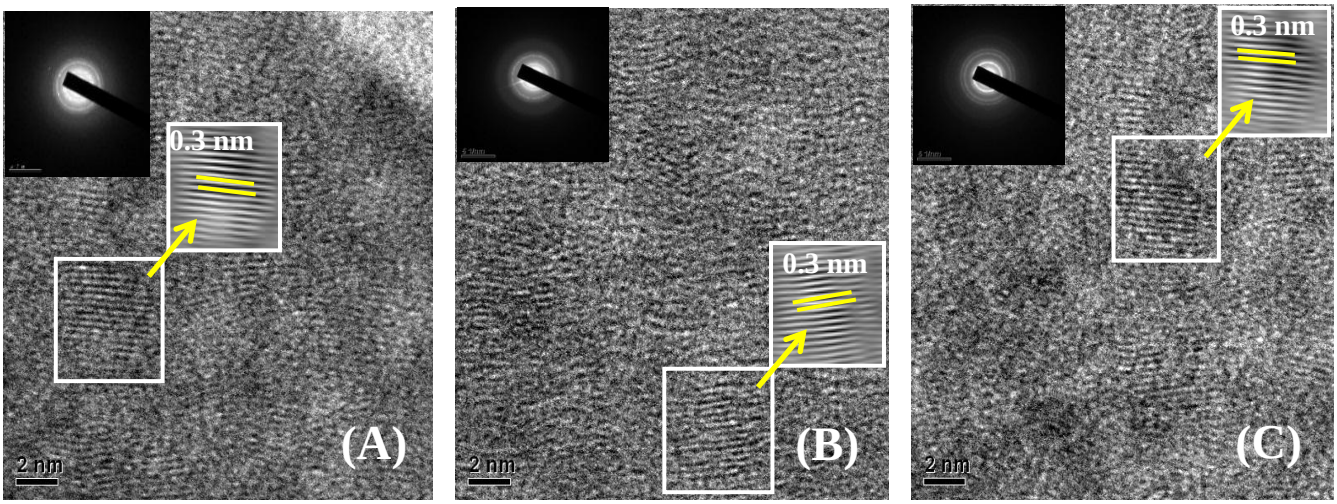

Figure S14. HRTEM (scale bar- 2 nm) and corresponding IFFT (in boxes) and SAED (inset; scale bar- 5 nm^{-1}) images of **(A)** cysteine capped ZnS Qdots, **(B)** HQ added ZnS Qdots and (**C**) ZnQ_2 added ZnS Qdots.

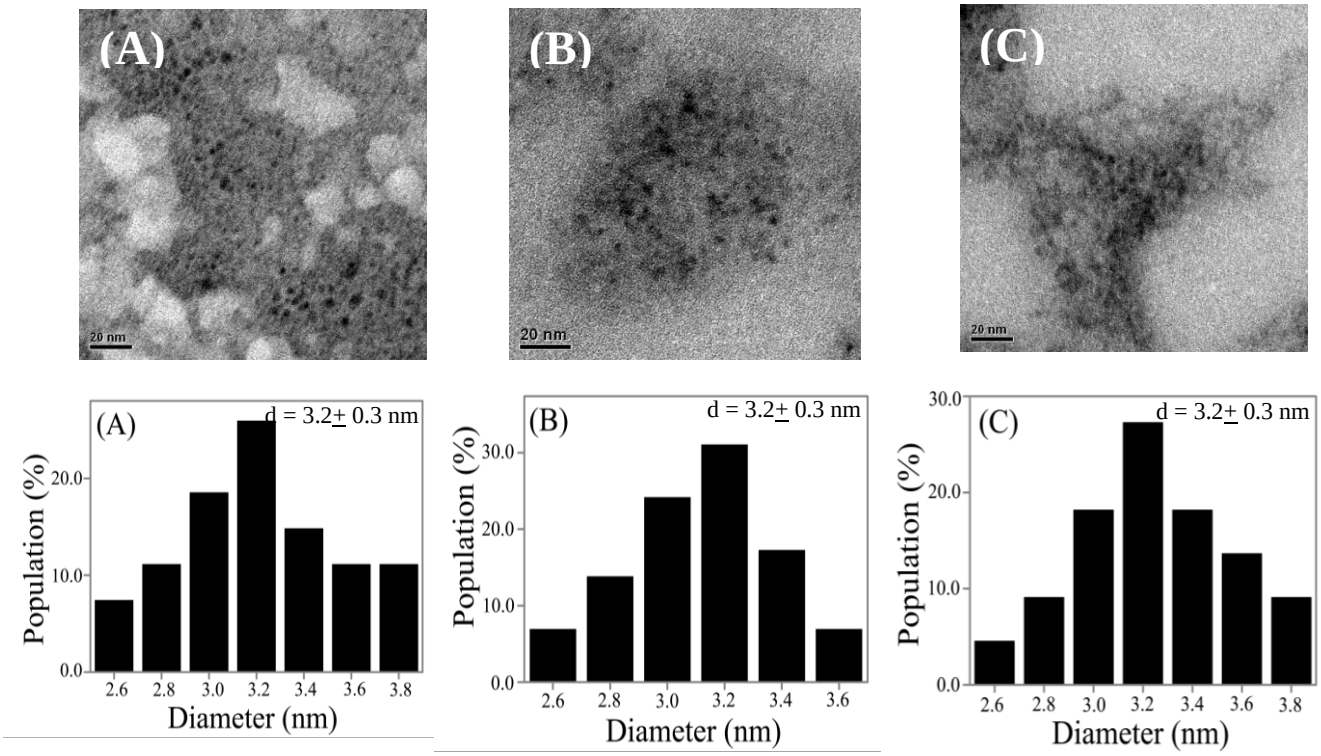

Figure S15. TEM images and corresponding particle size distribution of **(A)** as-synthesized cysteine capped ZnS Qdots; **(B)** HQ added ZnS Qdots and **(C)** ZnQ_2 added ZnS Qdots.

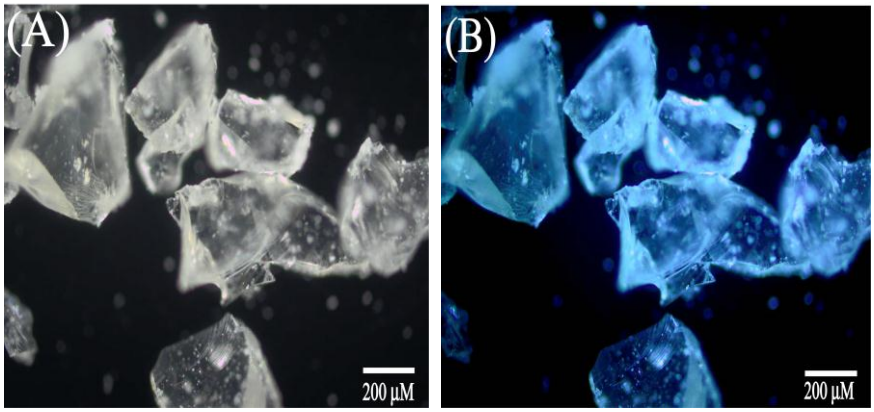

Figure S16: Microscopic images of cysteine capped ZnS Qdots in presence of **(A)** white and **(B)** UV light (λ_{ex} = 350 nm).

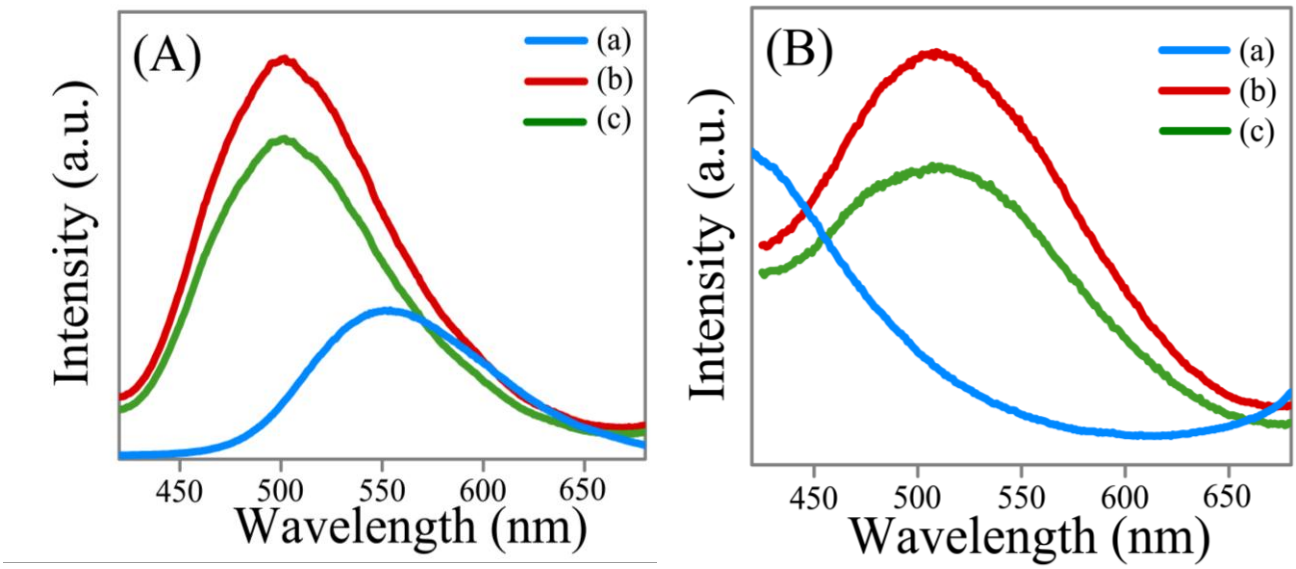

Figure S17. Emission spectra (λ_{ex}=361 nm) **(A)** before and **(B)** after heating at 350 ^{o}C of (a) ZnQ_2, (b) HQ added ZnS Qdots and (c) ZnQ_2 added ZnS Qdots.

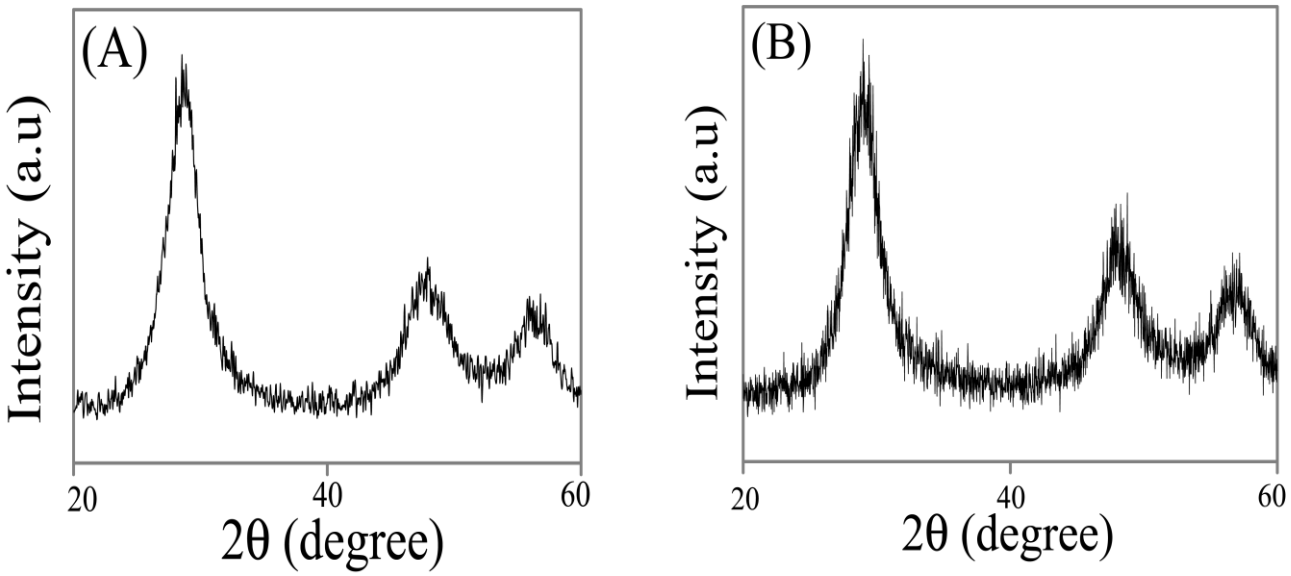

Figure S18: Powder X-ray diffraction pattern of **(A)** cysteine capped and (**B**) uncapped ZnS Qdots. The lattice planes corresponding to cubic ZnS crystals are identified.

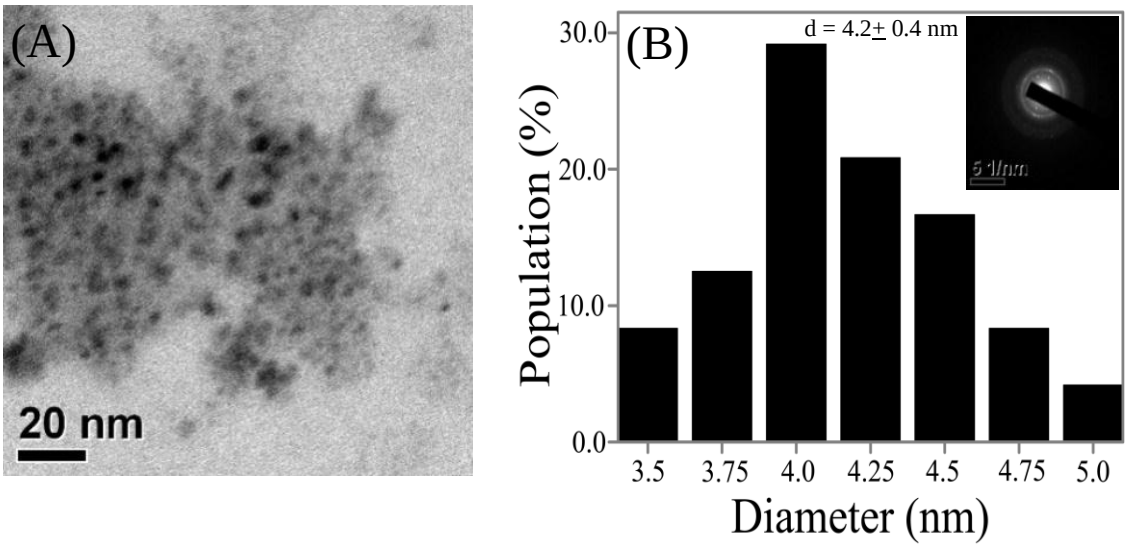

Figure S19: (A) TEM (scale bar-20 nm) image and **(B)** corresponding particle size distribution and SAED (inset; scale bar: 5 nm^{-1}) pattern of uncapped ZnS Qdots.

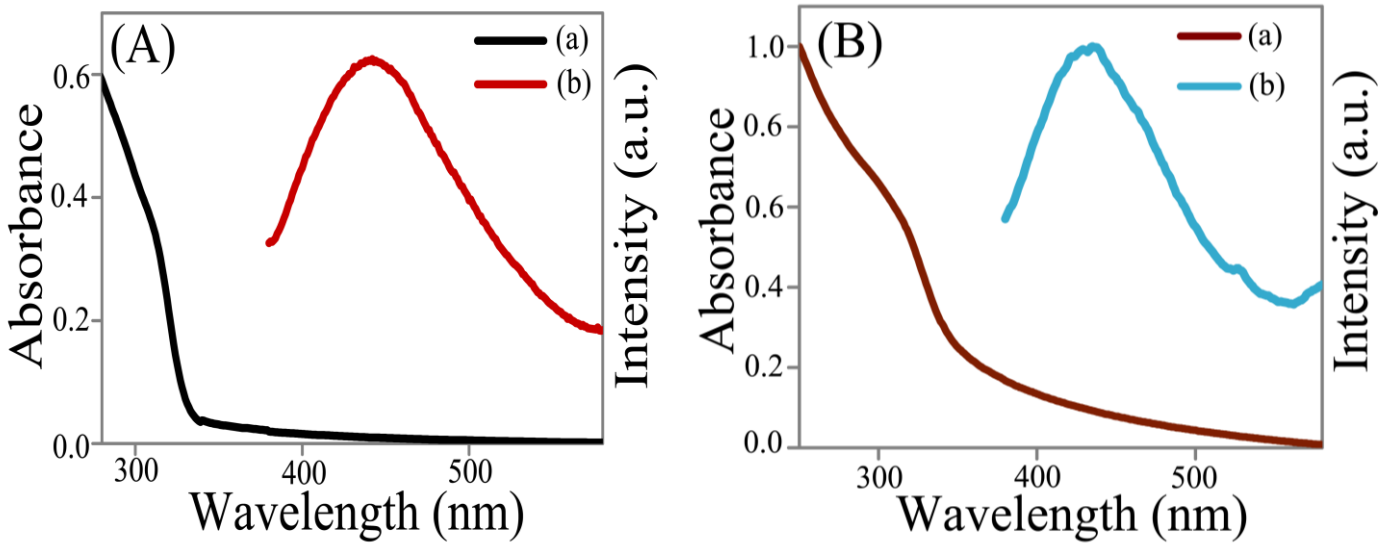

Figure S20: (A) UV-Vis and **(B)** emission spectra (λ_{ex}=361 nm; in water) of (a) cysteine capped and (b) uncapped ZnS Qdots.

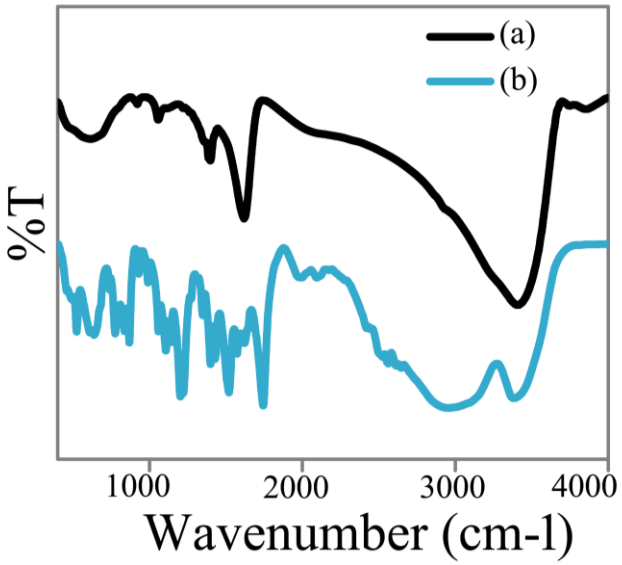

Figure S21: (a) FTIR spectra of cysteine capped ZnS Qdots and (b) cysteine.HCl.

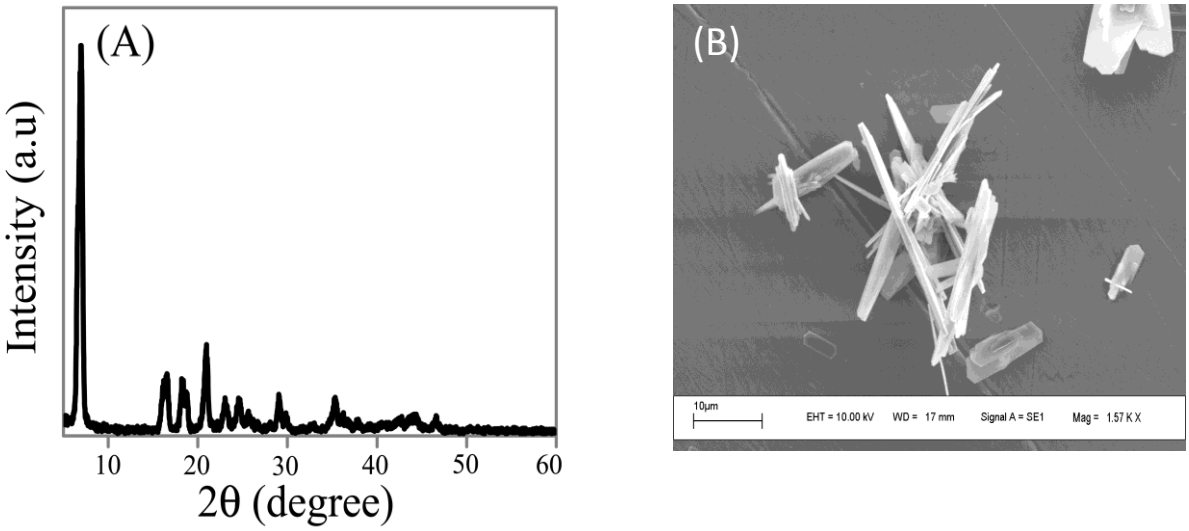

Figure S22: (A) Powder X-ray diffraction pattern and **(B)** SEM image (scale bar - 10 µM) of ZnQ_2.

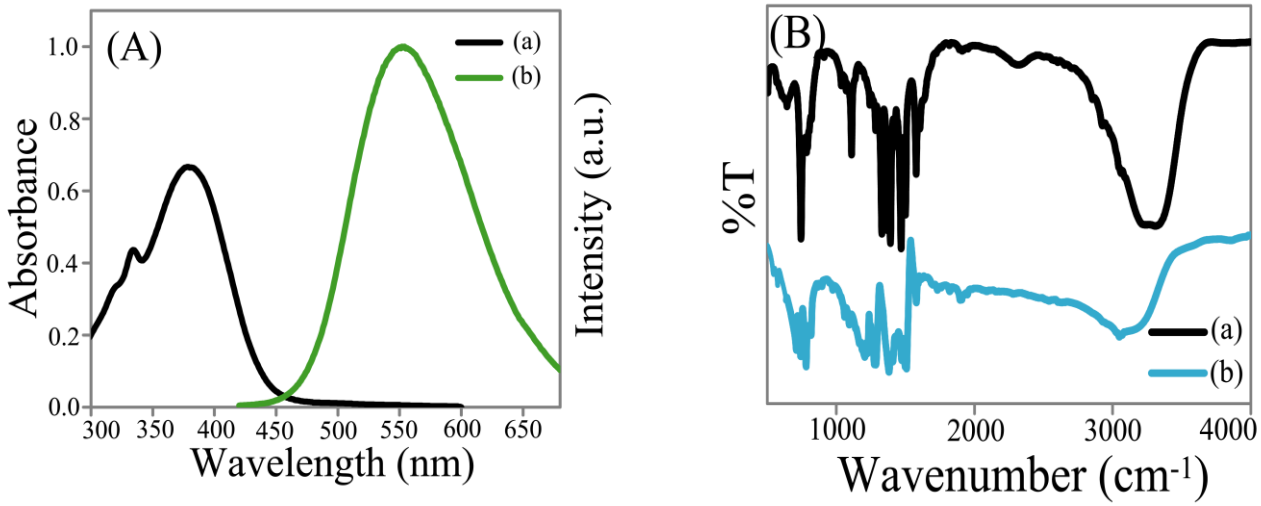

Figure S23: (A) (a) UV-Vis and (b) emission spectra (λ_{ex}=361 nm; in methanol) of $ZnQ_2.2H_2O$. **(B)** FTIR spectra of (a) $ZnQ_2.2H_2O$ and (b) 8-HQ.

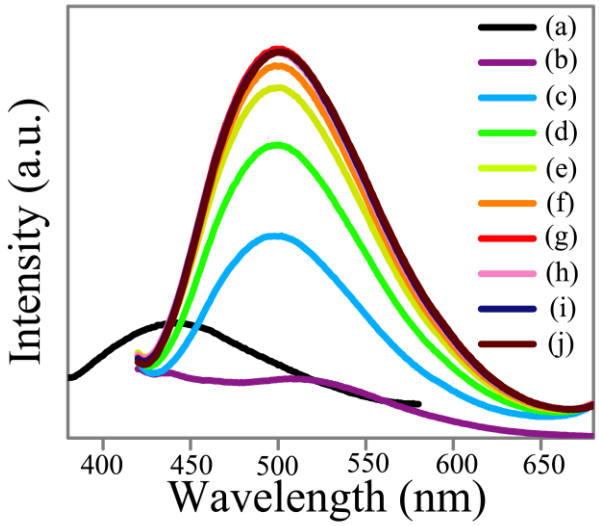

Figure S24. Emission spectra (λ_{ex} = 361nm) of (a) Qdots (λ_{ex} = 322 nm) in water, (b) 5.0 mM of 8-HQ in methanol and (c) 5.0 µL, (d) 10.0 µL, (e) 15.0 µL, (f) 20.0 µL, (g) 25.0 µL, (h) 30.0 µL, (i) 35.0 µL and (j) 40.0 µL of 5.0 mM 8-HQ (in methanol) added ZnS Qdots (2 mL) dispersion . The absorbance of the Qdots was 0.03 at 361 nm.

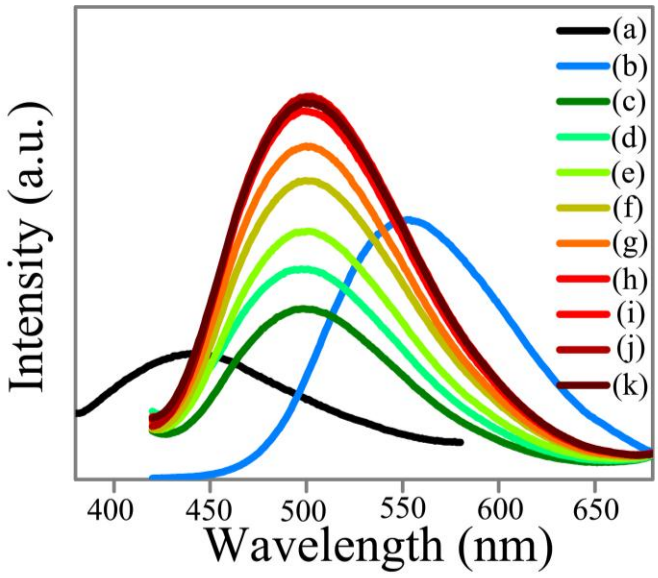

Figure S25. Emission spectra (λ_{ex} = 361nm) of (a) Qdots (λ_{ex} = 322 nm) in water, (b) 0.5 mM of ZnQ_2 in methanol and different amount (c) 10.0 μL, (d) 20.0 μL, (e) 30.0 μL, (f) 40.0 μL, (g) 60.0 μL, (h) 80.0 μL, (i) 100.0 μL, (j) 120.0 μL and (k) 140.0 μL of 0.5 mM of ZnQ_2 (in methanol) added ZnS Qdots (2 mL) dispersion. The absorbance of the Qdots was 0.03 at 361 nm.

Quantum Yield calculation with respect to quinine sulphate (QS) in 0.1 M H_2SO_4:

We have calculated quantum yield with respect to quinine sulphate using the formula,

$$Q_s = Q_R \times \frac{I_s}{I_R} \times \frac{A_R}{A_S} \times \frac{\eta_S^2}{\eta_R^2} \qquad (1)$$

Where, Q_S = quantum yield of sample; Q_R = quantum yield of reference; I_S = area under PL curve of sample; I_R = area under PL curve of reference; A_R = absorbance of the reference; A_S = absorbance of the sample; η_S = refractive index of sample; η_R = refractive index of reference. Q.Y. of quinine sulphate = 0.54 (54 %); Refractive Index: methanol = 1.328; water = 1.33. (The concentration of all samples and the reference quinine sulphate were adjusted so that the optical densities of all samples were 0.1 $\pm$ 0.01 at their corresponding excitation wavelength (i.e at 322 and 361 nm)).

Samples	Q.Y (%) with excitation at	
	322 nm	**361 nm**
(a) ZnS Qdots	0.3	-
(b) HQ	-	0.2
(c) ZnQ_2	-	0.9
(c) HQ added ZnS Qdots	0.16	3.2
(d) ZnQ_2 added ZnS Qdots	0.14	3.0

Table S1: Quantum yield (%) of (a) cysteine capped ZnS Qdots, (b) HQ, (c) ZnQ_2, (d) (c) HQ added ZnS Qdots and (d) ZnQ_2 added ZnS Qdots.

Table S2

(A) Decay parameters of the product following complexation between cysteine capped ZnS Qdots and 8-HQ or ZnQ_2, monitored at 308 nm (using LED)

Samples	A_1 (%)	τ_1 (ns)	A_2 (%)	τ_2 (ns)	A_3 (%)	τ_3 (ns)	τ_{av} (ns)	χ^2
ZnS Qdots	16.25	3.35	83.75	33.63	-	-	33.1	1.03
HQ added ZnS Qdots	3.88	2.178	43.59	6.05	52.54	13.49	11.4	1.02
ZnQ_2 added ZnS Qdots	3.93	0.789	40.56	5.88	55.52	14.18	12.2	1.04

(B) Decay parameters of complexation between cysteine capped ZnS Qdots and 8-HQ or ZnQ_2 monitored at 375 nm (using LASER).

Samples	A_1 (%)	τ_1 (ns)	A_2 (%)	τ_2 (ns)	A_3 (%)	τ_3 (ns)	τ_{av} (ns)	χ^2
ZnQ_2	100	2.47	-	-	-	-	2.47	1.03
HQ added ZnS Qdots	5.72	1.31	42.39	5.05	51.89	12.36	10.5	1.06
ZnQ_2 added ZnS Qdots	6.87	1.55	40.51	6.06	52.62	14.11	11.9	1.02

Decay profiles were fitted to a multi-exponential model:

$$I(t) = \sum_i \alpha_i \exp\left(-t/\tau_i\right) \quad (2)$$

Where, single, bi and tri exponential functions were used to fit respective emission with obtaining χ^2 close to 1.0. We also report intensity-averaged life times ($\boldsymbol{\tau_{av}}$) in Table S3, determined from the results of three exponential model using

$$\tau_{av} = \frac{\sum_i \alpha_i \tau_i^2}{\sum_i \alpha_i \tau_i} \quad (3)$$

Where, α_i and τ_i are the pre-exponential factors and excited-state luminescence decay time associated with the *i*-th component, respectively.

Table S3

Table S3: Fluorescence decrease rate (% per sec) of (a) Conventional organic dye (Rhodamine 6G) (b) HQ added ZnS Qdots (c) ZnQ_2 added ZnS Qdots and (d) ZnQ_2 complex.

Samples	Fluorescence decease rate (I/I_0) (% per sec)
Rhodamine 6 G	0.013
HQ treated ZnS Qdots	0.003
ZnQ_2 treated ZnS Qdots	0.004
ZnQ_2 complex	0.004

Expanded FTIR Figures:

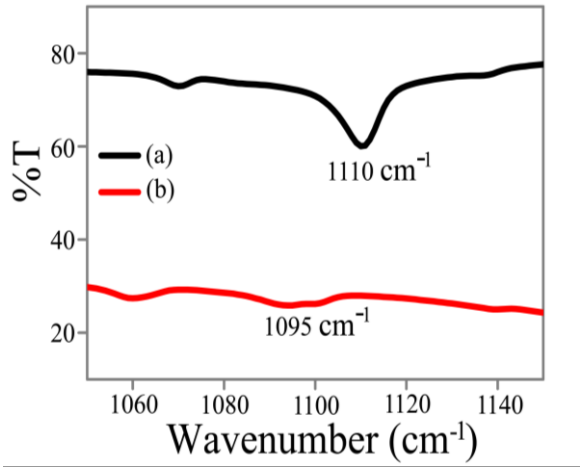

Figure S26: FTIR spectra (range: 1050-1150 cm^{-1}) of (a) ZnQ_2 and (b) 8-HQ.

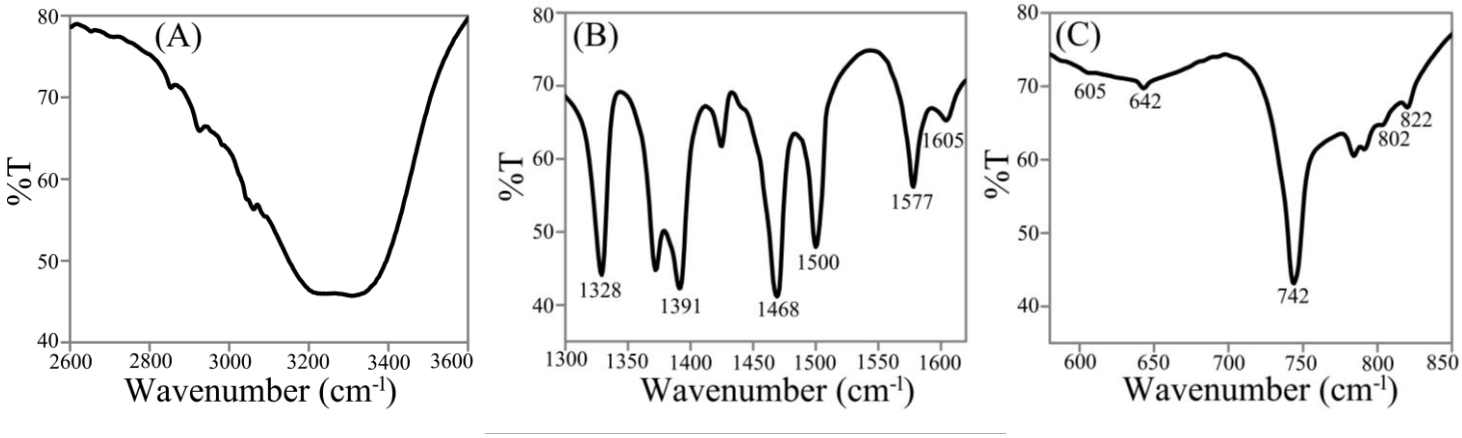

Figure S27: FTIR spectra of ZnQ_2. (**A**) range: 2600-3600 cm^{-1}, (**B**) range: 1300-1620 cm^{-1} and (**C**) range: 580-850 cm^{-1}.

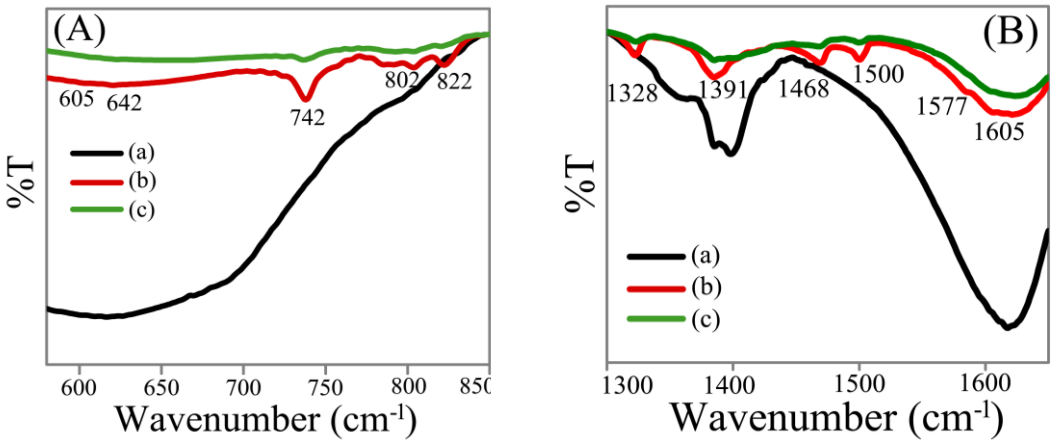

Figure S28: FTIR spectra in the (**A**) range: 580-850 cm^{-1} and (**B**) range: 1300-1620 cm^{-1} of (a) ZnS Qdots (b) HQ added ZnS Qdots and (c) ZnQ_2 added ZnS Qdots.

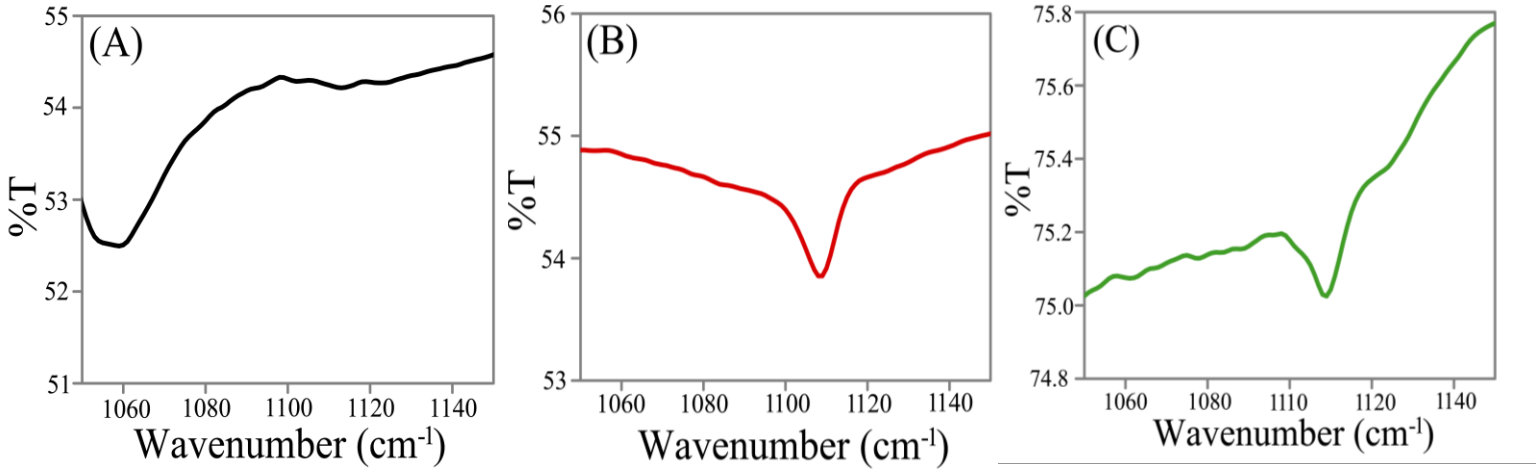

Figure S29: FTIR (range: 1050-1150 cm^{-1}) spectra of (**A**) ZnS Qdots, (**B**) HQ added ZnS Qdots and (**C**) ZnQ_2 added ZnS Qdots.

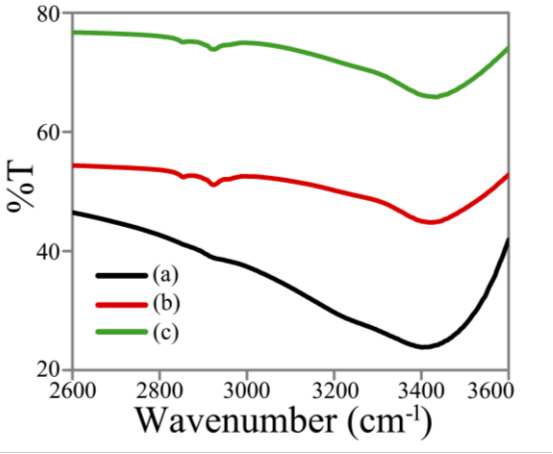

Figure S30: FTIR (range: 2600-3600 cm^{-1}) spectra of (a) ZnS Qdots, (b) HQ added ZnS Qdots and (c) ZnQ_2 added ZnS Qdots.

Wave number (Cm^{-1})	Functional groups	(a) ZnQ_2	(b) ZnS Qdots	(c)HQ added ZnS Qdots	(d) ZnQ_2 added ZnS Qdots
1605	C-C/C-N stretching	P	A	P	P
1577	C-C/C-N stretching	P	A	P	P
1500	Pyridyl group of HQ	P	A	P	P
1468	Phenyl group of HQ	P	A	P	P
1328	C-H bending	P	A	P	P
1110	-C-O-Zn Stretching	P	A	P	P
822	C-H out plane wagging	P	A	P	P
802	C-H out plane wagging	P	A	P	P
742	C-H out plane wagging, in plane ring deformation	P	A	P	P
642	in-plane ring deformation	P	A	P	P
605	in-plane ring deformation	P	A	P	P

*P: Present and A: Absent

Table S4: Tabulated FTIR wave number vs functional groups of (a) ZnQ_2, (b) cysteine capped ZnS Qdots, (c) HQ added ZnS Qdots and (d) ZnQ_2 added ZnS Qdots.

Samples	I_{3300} : I_{1110}
(a)	No significant peak at 1110 cm^{-1}
(b)	0.70
(c)	0.88
(d)	0.92

Table S5: Tabulated intensity ratio of 3333 cm^{-1} band to 1110 cm^{-1} band of (a) cysteine capped ZnS Qdots, (b) ZnQ_2, (c) HQ added ZnS Qdots and (d) ZnQ_2 added ZnS Qdots.

Explanation for FTIR Graphs:

The C-O stretching frequency observed in the free oxine molecule at 1095 cm^{-1}, shifted to higher frequencies in all the metal complexes giving a strong absorption band at 1110 cm^{-1} (-C-O-M) (Figure S25). This clearly indicates the coordination of HQ to Zn^{2+} ion in these complexes. The bands at 1605, 1577, 1391 and 1328 cm^{-1} are assigned to the quinoline group of ZnQ_2. The pyridyl and phenyl groups in ZnQ_2 are easily identified by presence of 1500 cm^{-1} and 1468 cm^{-1} bands respectively. Specifically, the presence of C-C/C-N stretching, C-H bending peaks at 1500, 1465, 1322 cm^{-1}, C-H out plane wagging at 822, 800, 742 cm^{-1} and in-plane ring deformation at 742, 642 and 605 cm^{-1} in the ZnQ_2 indicated that HQ was successfully coordinated to Zn^{2+} ion to form complex.[3] (Figure S26 and Table S3) Moreover, it is earlier reported that the intensity ratio of 3333 cm^{-1} (3μ) band to 1110 cm^{-1} (9μ) is commonly used to identify the number of water molecules in metal quinolates. The intensity ratio (3333 cm^{-1} /1110 cm^{-1}) is 0.30 $\pm$ 0.05 for one and 0.60 $\pm$ 0.05 for two molecules of water per molecule of quinolate.[3, 7] Here, the intensity ratio was found to be 0.70 which is slightly higher than the expected value for presence of two molecules of water for ZnQ_2 complex, which indicates the

possible presence of two water molecules in the complex.(Table S4) This indicates that the formation of $ZnQ_2.2H_2O$ complex.

Similarly, for HQ added ZnS Qdots and ZnQ_2 added ZnS Qdots the same characteristic peaks as in ZnQ_2 (which were absent in ZnS Qdots) were observed and the intensity ratios of 3333 cm^{-1} (3μ) band to 1110 cm^{-1} (9μ) band were found to be 0.88 and 0.92, respectively. This supported the formation of ZnQ_2 over the surface of ZnS Qdots. (Figure S27-30 and Table S3, S4) The difference from ZnQ_2 could be due to the presence of S^{2-} which might be attached to the axial position replacing one water molecule of the hexagonal complex.

References:

[1] A. Jaiswal, S. S. Ghosh and A. Chattopadhyay, *Langmuir*, 2012, **28**, 15687.

[2] J. Nanda, S. Sapra, D. D. Sarma, N. Chandrasekharan and G. Hodes, *Chem Mater.*, 2000, **12**, 1018.

[3] H. Pan, F. Liang, C. Mao, J. Zhu and H. Chen, *J. Phys. Chem. B*, 2007, **111**, 5767.

[4] Bing-she, H. Yu-ying, W. Hua, Z. He-feng, L. Xu-guang and C. Ming-wei, *Solid State Commun.* 2005, **136**, 318.

[5] R. Pohl and Jr P. Anzenbacher, *Org. Lett*., 2003, **5**, 2769.

[6] R. Pohl, V. A. Montes, J. Shinar and Jr P. Anzenbacher, *J. Org. Chem.*, 2004, **69**, 1723.

[7] J. P. Phillips and J. F. Deye, *Anal. Chim. Acta*, 1957, **17**, 231.